Available online at www.sciencedirect.com
ScienceDirect
Lithos 97 (2007) 289–306
LITHOS
www.elsevier.com/locate/lithos

Microstructures of olivine-plagioclase corona in meta-ultramafic rocks from Sefuri Mountains, NW Kyushu, Japan

T. Ikeda [a,*], T. Nishiyama [b], S. Yamada [a], T. Yanagi [a]

[a] Department of Earth and Planetary Sciences, Graduate School of Science, Kyushu University, 33 Hakozaki, Fukuoka, 812-8581 Japan
[b] Department of Earth and Environment, Kumamoto University, 2-39-1 Kurokami Kumamoto, 860-8555, Japan

Received 10 May 2006; accepted 18 December 2006
Available online 10 January 2007

Abstract

Two types of reaction rims occur between olivine and plagioclase in ultramafic rocks from the Sefuri Mountains, NW Kyushu, Japan, which were metamorphosed under granulite-facies conditions. One occurs as a thin film of orthopyroxene along the boundary between olivine and plagioclase (orthopyroxene zone). The other is composed of two zones: symplectite of calcic amphibole and spinel on the plagioclase-side (symplectite zone) and calcic amphibole with sporadic orthopyroxene on the olivine-side (tremolite zone). In the tremolite zone, calcic amphibole shows a systematic decrease in Al content and increase in Mg/(Fe+Mg) with decreasing distance from olivine. Local equilibria maintained during the diffusion-controlled corona-forming reaction enable us to apply equilibrium thermodynamics to calcic amphibole and adjacent orthopyroxene. An integrated formulation of the Gibbs method for an Fe–Mg exchange reaction constrains the equilibrium temperature recorded in the tremolite zone to be 600–710 °C. It is significantly lower than the temperature of the granulite-facies metamorphism (800–900 °C) estimated using conventional geothermobarometry. Except for H_2O, the association of calcic amphibole and spinel in the symplectite zone is chemically equivalent to the association of olivine, plagioclase and orthopyroxene that was stable before the corona formation. This suggests that the following orthopyroxene-consuming reaction describes the paragenetic change taking place between 800–900 °C and 600–710 °C, olivine+plagioclase+orthopyroxene+aqueous fluid=calcic amphibole+spinel. In contrast, the overall reaction inferred from microstructures produces orthopyroxene as well as calcic amphibole and spinel at the expense of olivine and plagioclase. This reaction requires removal mainly of MgO that is also responsible for destabilizing the local association of olivine and plagioclase. These features suggest that the presence of orthopyroxene as a product in the corona is not always indicative of an orthopyroxene-producing reaction being responsible for the change of paragenetic relation. Microstructural features should be carefully applied to infer the reaction describing paragenetic change by which we argue the *P–T* path of the rocks.
© 2006 Elsevier B.V. All rights reserved.

Keywords: Reaction microstructure; Olivine-plagioclase corona; Gibbs method; Symplectite

1. Introduction

Reaction microstructures, including coronas, represent common disequilibrium evidence in metamorphic and igneous rocks. Olivine-plagioclase coronas are common in metamorphosed mafic to ultramafic rocks,

* Corresponding author. Tel.: +81 926422649; fax: +81 926422684.
E-mail address: ikeda@geo.kyushu-u.ac.jp (T. Ikeda).

0024-4937/$ - see front matter © 2006 Elsevier B.V. All rights reserved.
doi:10.1016/j.lithos.2006.12.016

and have been extensively studied (e.g., Grieve and Gittins, 1975; Lamoen, 1979; Mongkoltip and Ashworth, 1983; Nishiyama, 1983; Grant, 1988; Ashworth et al., 1992; Ashworth and Sheplev, 1997). The precursors to the coronal assemblages are the simple assemblage, olivine and plagioclase. Nevertheless the coronas represent significant variation in mineral species and zonal sequence. These features have been explained in terms of diffusion-controlled processes proposed by Fisher (1973) and Joesten (1977) in either an open or a closed system in which local equilibrium was attained (e.g., Nishiyama, 1983; Ashworth and Birdi, 1990; Johnson and Carlson, 1990). In these processes, the ratio of the phenomenological coefficients is essential. The phenomenological coefficient depends on temperature, as is similar to the case of the diffusion coefficient of a single material. It is therefore important to know the temperature under which the diffusion-controlled reaction took place to form the coronas.

Temperature conditions of the corona formation have been, however, seldom constrained, except for Grieve and Gittins (1975) who applied a geothermometer to preexisting clinopyroxene and newly-formed orthopyroxene to estimate the upper limit of temperature. The presence of reaction microstructures indicates that the reaction has not been completed. This suggests that equilibrium has been attained not in the scale of the overall system but on a more local scale (cf. Nakamura, 2002). In addition, chemical reaction does not occur under the equilibrium condition but requires supersaturation to some extent to take place. Therefore analyses of the overall reaction based on equilibrium thermodynamics such as petrogenetic grid and thermodynamic calculation do not provide information on condition under which the reaction took place.

Recently, Ikeda (2004) proposed a thermodynamic formulation that evaluates difference in pressure and temperature between the different equilibrium states. This corresponds to the integrated formulation of the Gibbs method (Spear et al., 1982). This study applies the method to an olivine-plagioclase corona in meta-ultramafic rocks from the Sefuri Mountains, NW Kyushu, Japan, and estimates the temperature of the reaction based on the concept of local equilibrium. In addition, this study determines the overall open-system reaction that took place at this temperature. Combining the proposed overall reaction with the reaction that describes change of paragenetic relation, we emphasize the importance of removal of MgO to account for both the occurrence of orthopyroxene as a reaction product and the development of reaction rims between olivine and plagioclase.

2. Sample descriptions

2.1. Geological outline

The coronitic meta-ultramafic rocks occur in a small exposure of metamorphic rocks (2.3×1.0 km^2) within Cretaceous granitic rocks on the northern side of the Mt. Uki-dake, one of the peaks in the Sefuri Mountains, NW Kyushu, Japan (Fig. 1). The constituent lithology of this exposure includes pelitic, mafic, siliceous, calc-silicate and ultramafic rocks. The common occurrence of orthopyroxene in pelitic and mafic rocks suggests that the metamorphic grade belongs to the granulite facies (Yamada and Yanagi, 1986; Owada et al., 2005). The metamorphic conditions were estimated as 0.4–0.5 GPa, 800–900 °C by Owada et al. (2005) based on two-pyroxene and garnet–orthopyroxene geothermometers together with the garnet–orthopyroxene–plagioclase–quartz geobarometer. Owada et al. (2005) considered that the granulite–facies metamorphism preceded the intrusion of granitic rocks because orthopyroxene and clinopyroxene occurring in the vicinity of the boundary between the metamorphic rocks and granitic rocks are preferentially replaced by hornblende.

High-pressure type metamorphic rocks occur regionally in areas east of Fukuoka that have been formerly referred to as the Sangun Metamorphic Rocks (Fig. 1). They are recently re-defined as the 280–330 Ma Renge belt by Nishimura (1998). The metamorphic grade of the Renge belt belongs to the glaucophane–schists to epidote–amphibolite facies (Karakida, 1965; Nishimura, 1998). Some metamorphic rocks occur within the Cretaceous granitic rocks in-between the metamorphic exposure at Mt. Uki-dake and the areas belonging to the undisputed Renge belt (Fig. 1). They comprise rock types similar to the Renge belt, such as mafic and pelitic rocks with subordinate ultramafic, siliceous and calcareous rocks, but are metamorphosed under the amphibolite-facies conditions (Sugi, 1951; Matsumoto, 1958; Karakida, 1969, 1971; Owada et al., 2000). It is still controversial how to account for the similarity in rock type but distinction in metamorphic grade between rocks of the Renge belt and those within granitic rocks, including rocks at Mt. Uki-dake (e.g., Karakida, 1951; Inoue, 1961; Karakida, 1969; Owada et al., 2000).

This study deals with the boulders of ultramafic rocks collected in a stream on the northern slope of Mt. Uki-dake that were derived from the small exposure described by Owada et al. (2005) (Fig. 1).

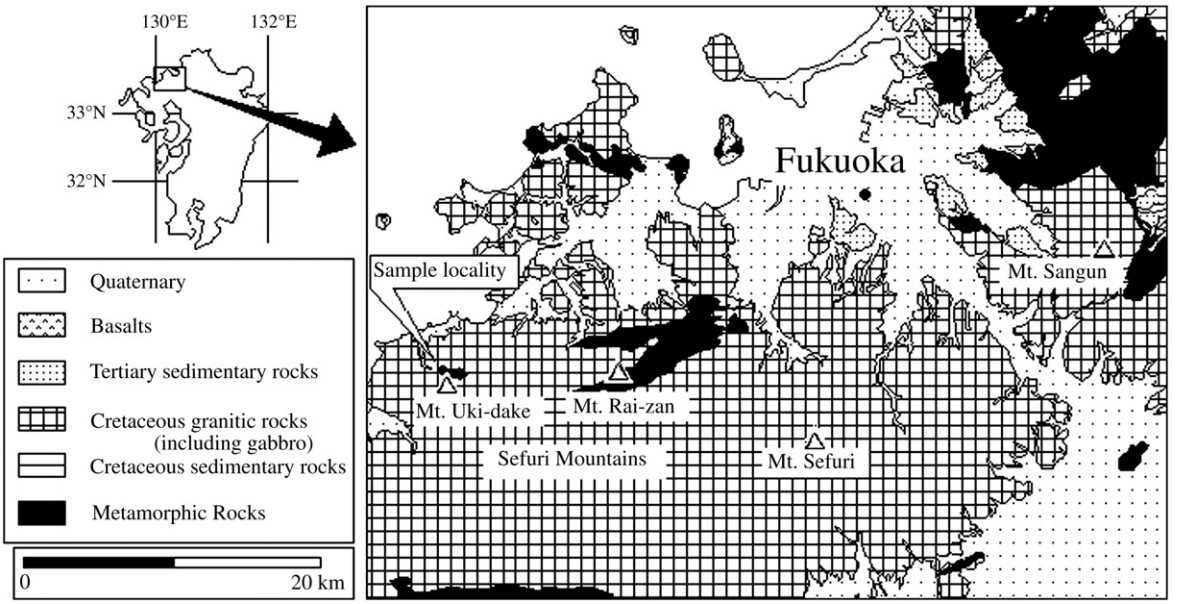


Fig. 1. Geological map of NW Kyushu, SW Japan, simplified after Karakida et al. (1994), showing the locality of samples investigated in this study.

2.2. Microstructure

The meta-ultramafic rocks comprise two domains with different mineral assemblages and microstructures, referred to as the calcic amphibole–orthopyroxene (Cam–Opx) domain and olivine–plagioclase (Ol–Pl) domain. The Cam–Opx domain is composed mainly of fine-grained (<0.5 mm) equigranular calcic amphibole and orthopyroxene together with rare chromian spinel. Calcic amphibole and orthopyroxene show polygonal shapes with flat grain-boundaries (Fig. 2a), i.e., equigranular-polygonal type of Moore (1970). Chromian spinel is embedded in calcic amphibole as fine-rounded grains, and locally includes magnetite (Fig. 2b).

The Ol–Pl domain consists mainly of coarse olivine, spinel, plagioclase and ilmenite together with poikiloblasts of calcic amphibole and subordinate orthopyroxene (Fig. 2c–e). Biotite is also present rarely. This domain represents two types of reaction rims between olivine and plagioclase. One is a thin film (<70 μm thick) composed of polycrystalline orthopyroxene at the boundary between olivine and plagioclase, which is referred to as the orthopyroxene zone (Fig. 2f). The other consists of two zones: symplectite zone on the plagioclase-side and tremolite zone on the olivine-side (Fig. 2g), which is more common than the first type of the reaction rims. The symplectite zone is composed of vermicular grains of green spinel embedded in calcic amphibole. Long axes of most vermicular spinel are orientated approximately perpendicular to the boundary between plagioclase and the symplectite zone. The tremolite zone consists mainly of calcic amphibole with sporadic orthopyroxene that is in direct contact with either spinel in the symplectite zone or olivine (Fig. 2g). Calcic amphibole in the tremolite zone has the same crystallographic orientation as that in the symplectite zone, and no Becke line is recognized between the two amphiboles under the microscope. Both the symplectite zone and tremolite zone represent significant variation in thickness, and are thicker than the orthopyroxene zone.

Plagioclase grain is as coarse as 2 mm long in maximum and occurs either as individual crystals or as polycrystalline aggregates. It is commonly twinned and locally includes rounded orthopyroxene (Fig. 2f), suggesting that orthopyroxene predated plagioclase. The boundary between the crystals of plagioclase in the aggregates is flat or smoothly curved in contrast to the shape of the individual grain and aggregates that is strongly curved and irregular (Fig. 2e). Grains of plagioclase are mostly armoured by either the orthopyroxene zone or the symplectite zone, and are locally in contact with orthopyroxene in the matrix that is fine (<0.2 mm) and polygonal. Orthopyroxene in the orthopyroxene zone can be easily distinguished from that in the matrix based on the restricted occurrence at the boundary between olivine and plagioclase, and based on a steep compositional gradient within the grain, as will be described later.

Calcic amphibole is colorless to pale green in both the Ol–Pl domain and Cam–Opx domain. In the matrix

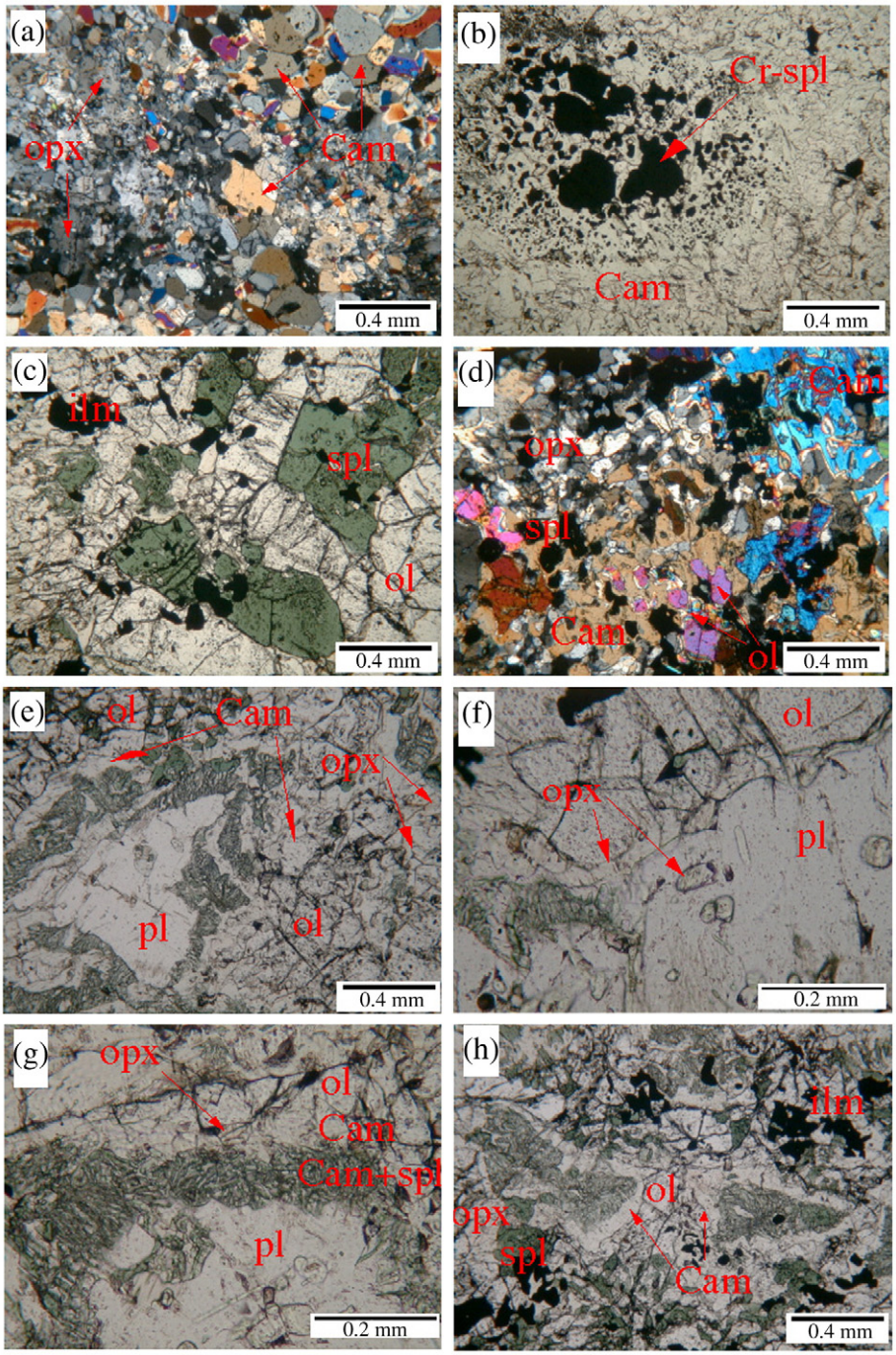


Fig. 2. Photomicrographs showing mode of occurrence of the constituent minerals of the meta-ultramafic rock. (a) and (b) from the Cam–Opx domain and (c) to (h) from the Ol–Pl domain. All photographs in plane-polarized light except for (a) and (d) that are in crossed-polarized light. a) Equigranular calcic amphibole (Cam) and orthopyroxene (opx). (b) Fine inclusions of chromian spinel (Cr-spl) within calcic amphibole. (c) Coarse grains of spinel (spl), olivine (ol) and ilmenite (ilm). (d) Orthopyroxene and poikiloblasts of calcic amphibole including olivine and spinel. (e) Coarse plagioclase (pl) surrounded by vermicular aggregates of spinel. (f) Thin orthopyroxene zone occurring between olivine and plagioclase. (g) Development of tremolite zone on the olivine-side and symplectite zone composed of spinel and calcic amphibole on the plagioclase-side. Sporadic occurrence of orthopyroxene within the tremolite zone. (h) Poikiloblasts of calcic amphibole including vermicular aggregates of spinel.

of the Ol–Pl domain, it commonly occurs as poikiloblasts up to 3 mm (Fig. 2d). The poikiloblasts include commonly rounded grains of green spinel (<0.2 mm) and, locally, orthopyroxene. They also contain rounded grains of olivine and vermicular aggregates of green spinel, which are spatially separated from each other (Fig. 2d, h). Plagioclase occasionally occurs at the centre of these spinel aggregates. The spatially close association of plagioclase and vermicular spinel aggregates within the poikiloblasts mimics the association of the symplectite zone around plagioclase. The spinel-free domain of poikiloblasts close to olivine corresponds to the tremolite zone adjacent to olivine. Grains of olivine spatially close to each other in the poikiloblasts have the same crystallographic orientation (Fig. 2d). Some grains of calcic amphibole in the symplectite zone and tremolite zone have the same crystallographic orientation with the poikiloblasts. These features suggest that poikiloblasts of calcic amphibole were formed at the expense of olivine and plagioclase.

Spinel in the matrix of the Ol–Pl domain occurs either as vermicular grains less than 5 μm width or as polygonal to rounded grains up to 0.8 mm in diameter (Fig. 2c). It is mostly green, and rarely brownish green at the centre of coarse grains. Polygonal to rounded spinel is in contact with olivine with a smoothly curved boundary. This suggests that the polygonal to rounded spinel coexisted with olivine before formation of the reaction rims, while the vermicular spinel was a product of the reaction.

Ilmenite is rounded to irregular and shows various grain size up to 0.6 mm (Fig. 2c, h). It occurs not only in the matrix closely associated with coarse olivine and spinel, but also as inclusions in olivine, spinel and poikiloblasts of calcic amphibole.

In both domains, orthopyroxene is rarely replaced by cummingtonite and chlorite in part. Olivine is also rarely replaced by chlorite in part. However, the modal abundance of such minerals indicative of secondary origin is negligibly small.

2.3. Mineral compositions

The chemical compositions of constituent minerals of a meta-ultramafic rock (#FK97-19) were determined by a scanning electron microscope (JEOL 5800LV) combined with an energy dispersive analytical system (Link ISIS) at Kyushu University. A 20 kV accelerating voltage, a 0.5 nA beam current and a 100 s livetime were employed. The element standards used in this study are jadeite for Na, oxides for Mg, Al, Si, potassium bromide for K, calcium fluoride for Ca and metals for Ti, Mn and Fe. The analytical precision 1σ is within 5% for elements of which oxide content exceeds 1 wt.%, while precisions for Na, Ti in calcic amphibole and Ca in orthopyroxene are 12, 22 and 21%, respectively.

Ferric contents in olivine and orthopyroxene based on stoichiometry are negligible. Those in spinel and ilmenite estimated from stoichiometry are less than 28% and 15% in atomic ratio of total iron, respectively. All analyses of calcic amphibole contain FeO as low as 3.1 to 5.6 wt.%, assuming total iron to be ferrous, which corresponds to the iron content less than 0.66 based on 23 oxygen. Application of the method to estimate ferric content proposed by Holland and Blundy (1994) and Dale et al. (2000) to these iron-poor analyses provides relative uncertainties as large as ca. 100%. No systematic difference in ferric estimation is recognized among calcic amphiboles with different mode of occurrence. The ferric-free assumption satisfies the constraints of the method within the uncertainties derived from analytical errors. Therefore this study treats calcic amphibole as ferric-free. The change in the Al content of calcic amphibole caused by treating iron either as ferric or ferrous is less than 0.03 per formula unit, which is negligible as compared with analytical errors. In contrast, Mg/(Fe+Mg) strongly depends on this assumption, where Fe denotes ferrous iron hereafter. The effect of this assumption on temperature estimation will be discussed later.

2.3.1. Calcic amphibole

Most calcic amphibole in the sample belongs to magnesiohornblende based on the classification of Leake et al. (1997), except for those in the tremolite zone and in part in the symplectite zone that are classified to tremolite. Calcic amphibole in the tremolite zone shows significant compositional variation, i.e., the Al content decreases and Mg/(Fe+Mg) increases towards olivine (Figs. 3a and 4). The composition of calcic amphibole in the symplectite zone is approximately constant (Fig. 4). No gap in composition of calcic amphibole is recognized at the boundary between the two zones. These amphiboles are virtually Na-free and show a chemical variation that is well explained by the tschermak substitution (Fig. 4).

Poikiloblasts of calcic amphibole in the matrix of the Ol–Pl domain show a feature similar to calcic amphibole in the tremolite zone, such that Al decreases and Mg/(Fe+Mg) increases in the vicinity of olivine. The compositions of poikiloblasts next to olivine are similar to those adjacent to olivine in the tremolite zone (Fig. 4). Poikiloblasts apart from olivine contain Na less than 0.8 wt.%, and their chemical variation is explained by the tschermak and edenite substitutions.

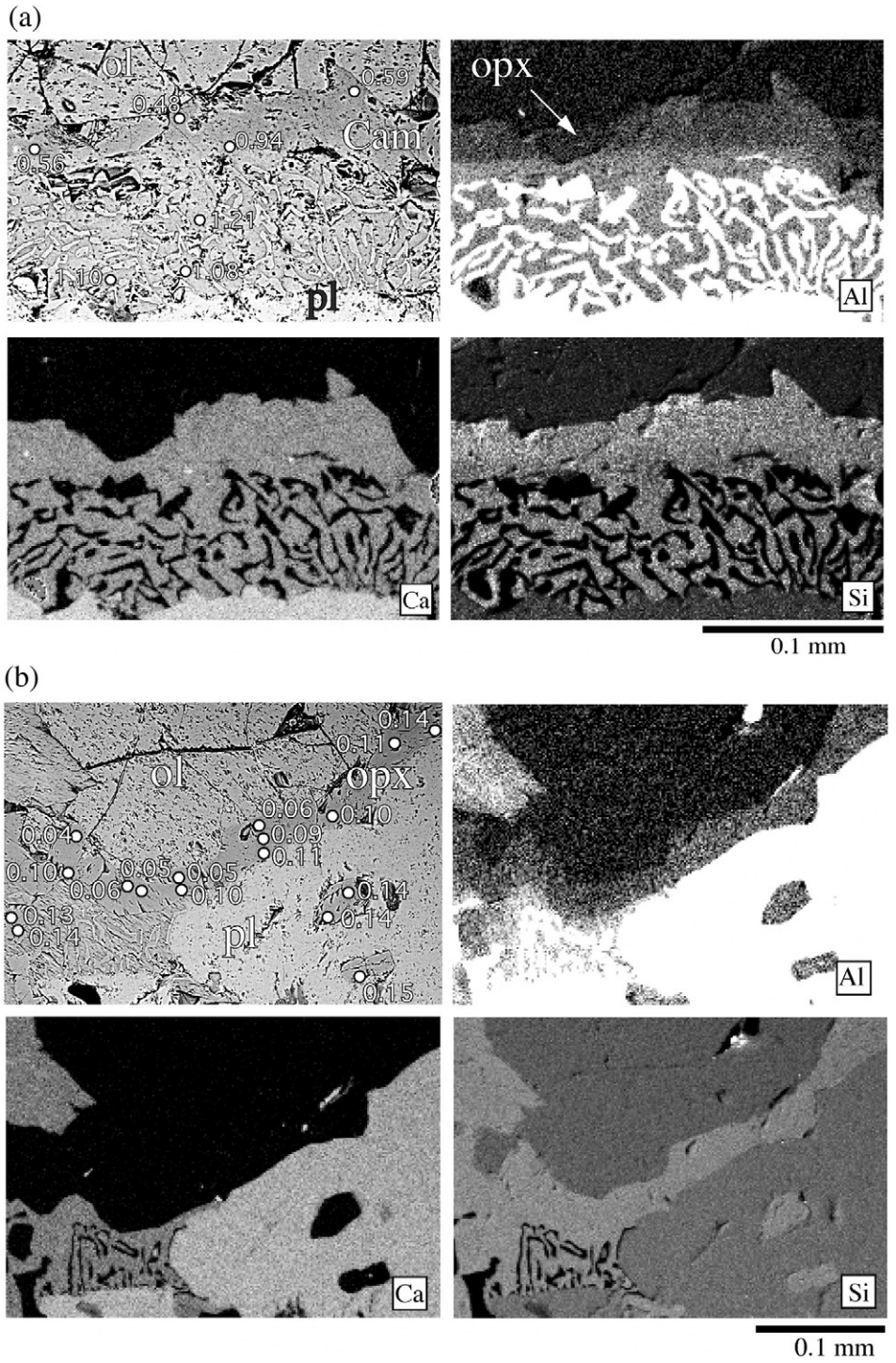


Fig. 3. Backscattered electron images (BEI) and X-ray image maps with respect to Ca, Al and Si. (a) and (b) are details of Fig. 2g and f, respectively. Numbers in the BEIs in (a) and (b) show the Al contents of calcic amphibole based on 23 oxygen and those of orthopyroxene based on 6 oxygen, respectively. Abbreviations: Cam, calcic amphibole; ol, olivine; opx, orthopyroxene; pl, plagioclase.

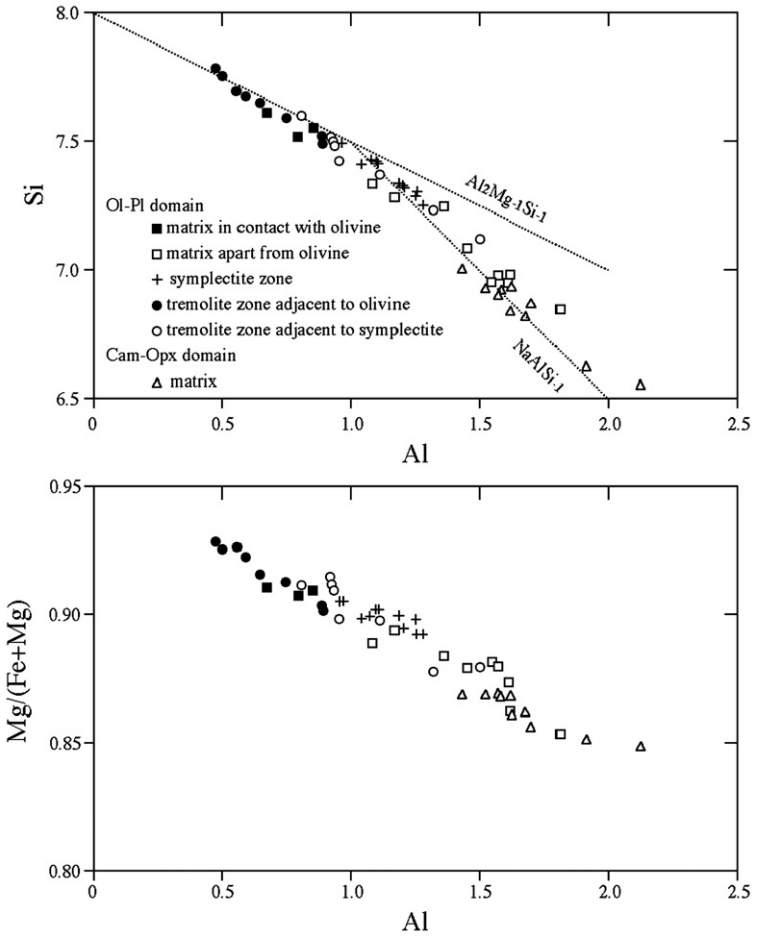


Fig. 4. Composition of calcic amphibole in terms of Si and Mg/(Fe+Mg) versus Al on the basis of 23 oxygen.

Calcic amphibole in the Cam–Opx domain is enriched in Al and contains Na as low as 0.8 wt.% (Table 1). Significant zoning was not detected. The Al contents differ in different grains, of which variation is accounted for by the tschermak and edenite substitutions (Fig. 4). This may be ascribed to local variation of the bulk composition, as discussed later.

2.3.2. Orthopyroxene

Grains of orthopyroxene in the matrix of Ol–Pl domain and those included in plagioclase have similar compositions that are enriched in Al up to 0.15 on the basis of 6 oxygen and Mg/(Fe+Mg) of 0.87 (Table 2). In contrast, orthopyroxene in the orthopyroxene zone and in the tremolite zone represents a significant chemical variation, where Al increases with increasing distance from olivine (Fig. 3b). These chemical variations in the sample are explained by the tschermak substitution with Mg/(Fe+Mg) being mostly constant as 0.87 (Fig. 5).

Orthopyroxene in the Cam–Opx domain is homogeneous. It is depleted in Al and similar in Mg/(Fe+Mg) as compared with those in the matrix of the Ol–Pl domain (Table 2).

2.3.3. Spinel

Grains of green spinel have similar compositions irrespective of difference in shape, vermicular or rounded to polygonal. Furthermore, the vermicular aggregates in the symplectite zone have compositions similar to those in the poikiloblasts of calcic amphibole. The Cr and Fe^{3+} contents of these green spinel are as low as 0.01 and 0.09 on the basis of 4 oxygen, respectively. TiO_2 is not detected. Therefore green spinel can be regarded as spinel (*sensu stricto*)–hercynite solid solution, in which Mg/(Fe+Mg) ranges from 0.75 to 0.78.

Brownish-green spinel, occurring sporadically at centre of coarse grains, contains Cr and Fe^{3+} up to 0.23 and 0.13 based on 4 oxygen, respectively. It shows Mg/

Table 1
Calcic amphibole analyses

Domain	Cam–Opx domain						Ol–Pl domain														
occurrence	Matrix						Tremolite zone									Symplectite zone			Matrix		
analysed point	Hbl-6	Hbl-7	Hbl-11	Hbl-16	Hbl-17	Hbl-19	Hbl-27	Hbl-28	Hbl-29	Hbl-32	Hbl-33	Hbl-43	Hbl-44	Hbl-48	Hbl-50	Hbl-4	Hbl-29	Hbl-36	Hbl-50	Hbl-21	Hbl-25
SiO_2	49.00	48.23	49.37	49.02	49.63	46.29	52.06	54.61	53.39	57.91	57.12	55.72	56.89	53.21	54.94	52.39	53.39	53.87	54.94	50.22	49.98
TiO_2	0.85	0.79	0.98	0.55	0.53	1.09	0.37	0.24	0.22							0.55	0.22			1.14	1.01
Al_2O_3	9.50	10.08	9.22	10.30	9.84	12.74	7.27	6.93	7.79	3.01	3.52	4.02	3.14	6.85	5.30	7.86	7.79	6.67	5.30	9.63	9.85
Cr_2O_3	0.83	1.00	0.45		0.34	0.26															
FeO	4.99	5.27	5.13	5.61	5.16	5.61	4.10	3.92	4.10	3.11	3.19	3.58	3.22	4.19	3.72	4.24	4.10	4.01	3.72	4.66	5.25
MnO	0.19			0.18									0.18							0.17	
MgO	18.47	18.25	18.99	18.66	18.97	17.57	19.37	20.33	20.10	22.61	22.29	21.58	22.25	20.48	20.77	19.71	20.10	20.04	20.77	18.95	18.41
CaO	12.60	12.58	12.56	12.54	12.51	12.67	12.94	13.13	13.10	12.68	13.33	12.89	12.48	12.58	13.03	12.81	13.10	13.06	13.03	12.85	12.82
Na_2O	0.76	0.75	0.74	0.80	0.67	0.81														0.43	
K_2O	0.18	0.20	0.14	0.12		0.19	0.14		0.19								0.19	0.12			0.31
Total	97.37	97.15	97.58	97.78	97.65	97.23	96.25	99.16	98.89	99.32	99.45	97.79	98.16	97.31	97.76	97.56	98.89	97.77	97.76	98.05	97.63
Si	6.902	6.822	6.928	6.874	6.939	6.555	7.311	7.411	7.291	7.787	7.699	7.650	7.755	7.371	7.554	7.252	7.291	7.427	7.554	6.973	6.981
Ti	0.090	0.084	0.103	0.058	0.056	0.116	0.039	0.025	0.023							0.057	0.023			0.119	0.106
Al	1.577	1.680	1.525	1.702	1.621	2.126	1.203	1.108	1.254	0.477	0.559	0.650	0.504	1.118	0.859	1.282	1.254	1.084	0.859	1.576	1.622
Cr	0.092	0.112	0.050		0.038	0.029															
Fe	0.588	0.623	0.602	0.658	0.603	0.664	0.482	0.445	0.468	0.350	0.360	0.411	0.367	0.485	0.428	0.491	0.468	0.462	0.428	0.541	0.613
Mn	0.023			0.021									0.021							0.020	
Mg	3.879	3.848	3.972	3.901	3.954	3.709	4.055	4.113	4.092	4.533	4.479	4.417	4.522	4.229	4.257	4.067	4.092	4.119	4.257	3.922	3.834
Ca	1.902	1.907	1.888	1.884	1.874	1.922	1.947	1.909	1.917	1.827	1.925	1.896	1.823	1.867	1.920	1.900	1.917	1.929	1.920	1.912	1.919
Na	0.208	0.206	0.201	0.217	0.182	0.222														0.116	
K	0.032	0.036	0.025	0.021		0.034	0.025		0.033								0.033	0.021			0.055
Total	15.293	15.318	15.294	15.336	15.267	15.377	15.062	15.011	15.078	14.974	15.022	15.024	14.992	15.070	15.018	15.049	15.078	15.042	15.018	15.179	15.130
Mg/(Fe+Mg)	0.868	0.861	0.868	0.856	0.868	0.848	0.894	0.902	0.897	0.928	0.926	0.915	0.925	0.897	0.909	0.892	0.897	0.899	0.909	0.879	0.862

The formula is calculated based on 23 oxygen (anhydrous).

Table 2
Orthopyroxene analyses

Domain	Cam–Opx domain						Ol–Pl domain																	
occurrence	Matrix						Tremolite zone									Orthopyroxene zone			Matrix			Inclusions in plagioclase		
analysed point	Opx-2	Opx-3	Opx-6	Opx-7	Opx-8	Opx-9	Opx-12	Opx-13	Opx-14	Opx-16	Opx-17	Opx-18	Opx-19	Opx-44	Opx-45	Opx-11	Opx-29	Opx-34	Opx-1	Opx-9	Opx-32	Opx-22	Opx-27	Opx-31
SiO_2	55.96	55.98	56.59	53.66	55.30	55.26	56.61	55.59	57.32	58.16	57.33	57.61	57.50	56.28	55.33	56.66	56.38	56.48	54.64	55.26	55.94	54.96	55.44	55.30
TiO_2																			0.29					
Al_2O_3	2.05	1.77	1.66	2.68	2.42	2.90	3.29	3.47	2.20	1.66	1.34	1.64	1.79	2.77	3.84	2.37	2.54	2.21	3.98	2.90	3.41	3.68	3.51	3.85
Cr_2O_3	0.33	0.26			0.23	0.19														0.19				
FeO	9.04	8.88	9.11	8.58	8.82	8.94	8.43	8.90	8.46	8.52	8.14	8.70	8.72	8.83	8.88	8.57	8.41	8.55	9.00	8.94	8.93	8.96	8.94	8.78
MnO	0.19	0.18	0.24	0.20			0.31		0.19	0.35		0.25			0.18	0.19	0.25		0.28		0.28		0.25	
MgO	32.03	31.63	32.47	31.06	31.90	31.68	31.84	31.61	33.05	33.18	32.77	33.22	32.94	32.75	31.75	32.91	32.93	32.82	31.89	31.68	32.05	31.48	32.00	31.68
CaO	0.46	0.53	0.16	0.21	0.23	0.20	0.17	0.30	0.17	0.17	0.15	0.13	0.12	0.23	0.25	0.15	0.13	0.14	0.16	0.20	0.30	0.28	0.20	0.28
Total	100.06	99.23	100.23	96.39	98.90	99.17	100.65	99.87	101.39	102.04	99.73	101.55	101.07	100.86	100.23	100.85	100.64	100.20	100.24	99.17	100.91	99.36	100.34	99.89
Si	1.953	1.968	1.968	1.940	1.948	1.941	1.952	1.937	1.963	1.979	1.990	1.972	1.975	1.942	1.923	1.953	1.947	1.958	1.904	1.941	1.932	1.927	1.926	1.926
Ti																			0.008					
Al	0.084	0.073	0.068	0.114	0.100	0.120	0.134	0.142	0.089	0.067	0.055	0.066	0.072	0.113	0.157	0.096	0.103	0.090	0.163	0.120	0.139	0.152	0.144	0.158
Cr	0.009	0.007			0.006	0.005														0.005				
Fe	0.264	0.261	0.265	0.259	0.260	0.263	0.243	0.259	0.242	0.242	0.236	0.249	0.250	0.255	0.258	0.247	0.243	0.248	0.262	0.263	0.258	0.263	0.260	0.256
Mn	0.006	0.005	0.007	0.006			0.009		0.006	0.010		0.007			0.005	0.006	0.007		0.008		0.008		0.007	
Mg	1.667	1.657	1.684	1.674	1.675	1.659	1.637	1.642	1.687	1.683	1.696	1.695	1.687	1.684	1.645	1.691	1.695	1.696	1.656	1.659	1.650	1.645	1.657	1.645
Ca	0.017	0.020	0.006	0.008	0.009	0.008	0.006	0.011	0.006	0.006	0.006	0.005	0.004	0.009	0.009	0.006	0.005	0.005	0.006	0.008	0.011	0.011	0.007	0.010
Total	4.000	3.991	3.998	4.001	3.998	3.996	3.981	3.991	3.993	3.987	3.983	3.994	3.988	4.003	3.997	3.999	4.000	3.997	4.007	3.996	3.998	3.998	4.001	3.995
Mg/(Fe+Mg)	0.863	0.864	0.864	0.866	0.866	0.863	0.871	0.864	0.875	0.874	0.878	0.872	0.871	0.869	0.864	0.873	0.875	0.872	0.863	0.863	0.865	0.862	0.864	0.865

The formula is calculated based on 6 oxygen.

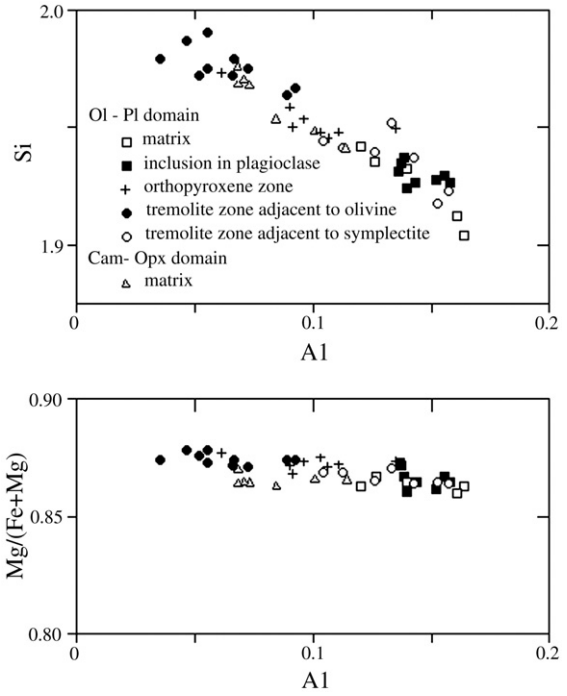


Fig. 5. Composition of orthopyroxene in terms of Si and Mg/(Fe+Mg) versus Al based on 6 oxygen.

(Fe+Mg) ranging from 0.65 to 0.75. TiO_2 was not detected (Table 3).

2.3.4. Olivine, plagioclase and other minerals

Olivine grains, both in the matrix and in the poikiloblasts of calcic amphibole, are chemically homogeneous with a forsterite content of 0.87. Plagioclase is homogeneous with composition of pure anorthite (Table 4). No X-ray peaks of Na and K were detected in the X-ray spectrum. The sporadic grains of plagioclase at the centre of vermicular aggregates of spinel within the poikiloblasts of calcic amphibole are also pure anorthite.

Ilmenite contains ferric iron in 10 to 15 mol% of total iron and has Mg/(Fe+Mg) of 0.23. Mg/(Fe+Mg) and Fe^{3+}/(Al+Cr+Fe^{3+}) of magnetite are 0.12 and 0.69, respectively. Biotite has Mg/(Fe+Mg) of 0.91 and contains Al and Ti of 2.86 and 0.12 on the basis of 22 oxygen, respectively. Cummingtonite replacing orthopyroxene has Mg/(Fe+Mg) of 0.89.

3. Thermodynamic consideration

The lines of microstructural and compositional evidence lead to the following interpretations. Olivine, plagioclase (pure anorthite), spinel, orthopyroxene and ilmenite were stable in the Ol–Pl domain before the formation of reaction rims, whereas calcic amphibole and orthopyroxene were equilibrated in the Cam–Opx domain. These two assemblages in the two domains are mutually consistent in terms of isophysical variation, as discussed later. In the Ol–Pl domain, a reaction took place between olivine and plagioclase, which caused a formation of two types of reaction rims together with poikiloblasts of calcic amphibole and vermicular spinel in the poikiloblasts. In contrast, calcic amphibole and orthopyroxene in the Cam–Opx domain show equigranular and polygonal microstructures without chemical

Table 3
Spinel analyses

Domain	Ol–Pl domain								
occurrence	Symplectite zone			Matrix			Inclusions in plagioclase		
analysed point	Spl-25	Spl-28	Spl-34	Spl-1	Spl-2	Spl-6	Spl-30	Spl-31	Spl-33
Al_2O_3	65.46	66.39	66.32	64.75	64.80	64.51	65.71	65.82	65.85
Cr_2O_3					0.20				
FeO	13.54	13.31	13.31	14.78	13.47	14.86	14.20	13.68	13.45
MnO				0.17		0.24			
NiO				0.39	0.27	0.33			
MgO	19.91	20.25	20.40	20.21	20.47	20.31	20.22	20.14	20.59
Total	98.91	99.95	100.03	100.30	99.21	100.25	100.13	99.64	99.89
Al	1.959	1.963	1.959	1.919	1.934	1.913	1.945	1.955	1.947
Cr					0.004				
Fe^{3+}	0.041	0.037	0.041	0.080	0.063	0.087	0.055	0.045	0.053
Fe^{2+}	0.246	0.243	0.238	0.231	0.222	0.226	0.243	0.243	0.230
Mn				0.004		0.005			
Ni				0.008	0.005	0.007			
Mg	0.754	0.757	0.762	0.758	0.772	0.762	0.757	0.757	0.770
Total	3.000	3.000	3.000	3.000	3.000	3.000	3.000	3.000	3.000

The formula is calculated based on 4 oxygen with 3 total cation to estimate ferric content.

Table 4
Olivine and plagioclase analyses

Analysed point	Ol-5	Ol-7	Ol-10	Pl-2	Pl-3	Pl-6	Pl-10
SiO_2	40.67	40.50	40.53	43.56	43.15	43.44	43.63
Al_2O_3				36.91	36.58	37.02	36.92
FeO	12.23	12.06	11.87				
MnO	0.27		0.23				
NiO	0.28	0.33					
MgO	47.28	47.27	46.72				
CaO				20.41	20.44	20.40	20.42
Total	100.73	100.16	99.35	100.88	100.17	100.86	100.97
Si	2.002	2.002	2.016	2.000	1.997	1.995	2.001
Al				1.997	1.995	2.004	1.996
Fe	0.504	0.499	0.494				
Mn	0.011		0.010				
Ni	0.011	0.013					
Mg	3.470	3.484	3.464				
Ca				1.004	1.014	1.004	1.004
Total	5.998	5.998	5.984	5.001	5.006	5.003	5.001

The formula is calculated based on 8 oxygen.

zoning, being indicative of preservation of equilibrium at high temperatures before the formation of reaction rims.

A large chemical gradient in calcic amphibole in the tremolite zone suggests that a diffusion process controlled the rate of the reaction. This has been well accepted in various types of olivine–plagioclase coronas (e.g., Nishiyama, 1983; Ashworth and Birdi, 1990; Johnson and Carlson, 1990). On the contrary, the chemical gradient is also expected when rate of dissolution of reactant minerals controls the reaction (e.g., Loomis, 1976). However, this process may be effective only at early stage of the reaction and may not remain to be the rate-control process during the entire stage of the corona formation. This study assumes that the diffusion controlled the rate of the reaction. Provided that the diffusion is the rate-controlling process, local equilibrium should be maintained (e.g., Fisher, 1978). The local equilibrium between calcic amphibole and orthopyroxene has been attained in the tremolite zone of the coronas when the reaction between olivine and plagioclase took place. The following Fe–Mg exchange reaction describes the equilibria between calcic amphibole and orthopyroxene in both the tremolite zone and the Cam–Opx domain.

$$\underset{\text{enstatite (en)}}{5\ Mg_2Si_2O_6} + \underset{\text{ferroactinolite (fact)}}{2\ Ca_2Fe_5Si_8O_{22}(OH)_2} = \underset{\text{ferrosilite (fs)}}{5\ Fe_2Si_2O_6} + \underset{\text{tremolite(tr)}}{2\ Ca_2Mg_5Si_8O_{22}(OH)_2} \quad (1)$$

Fig. 6 plots the distribution coefficient of Fe and Mg between calcic amphibole and orthopyorxene, K_D, defined as $(Mg/Fe)^{\text{calcic amphibole}}/(Mg/Fe)^{\text{orthopyroxene}}$, as a function of Al in octahedral site of calcic amphibole, Al^{vi}. We chose the paired analyses of calcic amphibole and orthopyroxene in the tremolite zone that are in contact with each other, based on the assumption of local equilibrium. In the Cam–Opx domain, the adjacent grains of calcic amphibole and orthopyroxene with homogeneous compositions were used. The pairs from both modes of occurrence show a similar feature that K_D decreases with increasing Al^{vi}, but K_D values in the Cam–Opx domain are significantly smaller than those in the tremolite zone at similar Al contents (Fig. 6). The Mg/Fe of orthopyroxene is approximately constant (Fig. 5), suggesting that the variation of K_D is largely ascribed to that of calcic amphibole. Calcic amphiboles in the tremolite zone and the Cam–Opx domain show the negative correlation between Mg/Fe and Al (Fig. 4). This feature of amphibole has been commonly described in

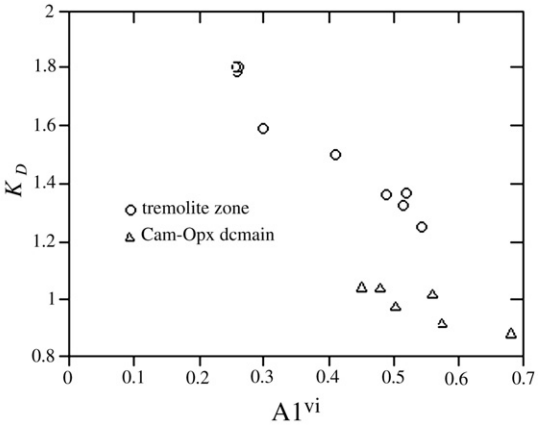


Fig. 6. K_D versus Al in octahedral site of calcic amphibole, Al^{vi}, where K_D is defined as $(Mg/Fe)^{\text{calcic amphibole}}/(Mg/Fe)^{\text{orthopyroxene}}$.

olivine-plagioclase coronas (e.g., Mongkoltip and Ashworth, 1983; Ashworth et al., 1992). We consider that the difference in K_D between the Cam–Opx domain and tremolite zone represents the temperature difference between the granulite-facies conditions and the corona-forming reaction. In contrast, the variation of K_D as a function of Al^{vi} in each mode of occurrence is ascribed to the isophysical variations. The validity of these considerations will be verified later by the temperature estimation based on reaction (1).

The K_D strongly depends on the ferric estimation of calcic amphibole, as cautioned before. There is no evidence to support a difference in oxygen fugacity between the tremolite zone and Cam–Opx domain. Introduction of ferric iron equally into calcic amphiboles of the two modes of occurrence increases K_D similarly to each other, which leads to the same features shown above. Nevertheless, ambiguity of ferric content in calcic amphibole has prevented the reaction (1) from establishing it as a geothermometer, and also makes it difficult to calculate thermodynamically using an internally consistent dataset. Alternatively we will evaluate reaction (1) based on the thermodynamic formulation of Ikeda (2004), as described below.

Owada et al. (2005) applied several geothermobarometers to pelitic and mafic gneisses in the small exposure on the northern side of Mt. Uki-dake (Fig. 1). The gneisses studied by Owada et al. (2005) show preferred orientation of constituent minerals that are chemically homogeneous without any alteration microstructures. Applying two-pyroxene geothermometer to mafic gneisses and garnet–orthopyroxene geothermometer together with garnet–orthopyroxene–plagioclase–quartz geobarometer to pelitic gneisses yields the conditions of the granulite–facies metamorphism as 0.4–0.5 GPa and 800–900 °C (Owada et al., 2005). The assemblage olivine+plagioclase+orthopyroxene+spinel, occurring in the Ol–Pl domain before corona formation, is stable under these conditions (cf. Tracy and Frost, 1991). We consider that the homogeneous calcic amphibole and orthopyroxene in the Cam–Opx domain with equigranular shapes were also equilibrated with each other under these conditions. A pair of analyses of calcic amphibole and orthopyroxene in the Cam–Opx domain that has K_D similar to the average K_D in the domain is chosen as a reference (analyses of Hbl-7 and Opx-2 in Tables 1 and 2, respectively), of which K_D is 0.98 (Fig. 6). We regard that the reference pair was equilibrated at 0.5 GPa and 850 °C taking the average of estimation by Owada et al. (2005).

The temperature conditions of other pairs, T_1, are obtained as a function of its pressure, P_1, by solving the following equation that describes the relation between equilibrium constant of reaction (1), K_{P_1,T_1}, at P_1-T_1 and the constant, K_{P_0,T_0}, at $P_0=0.5$ GPa and $T_0=850$ °C (Ikeda, 2004).

$$RT_1\ln K_{P_1,T_1} = RT_0\ln K_{P_0,T_0} + \int_{T_0}^{T_1}\Delta S\,dT - \int_{P_0}^{P_1}\Delta V\,dP \quad (2)$$

Parameters, R, ΔS and ΔV denote the universal gas constant, entropy of the reaction and volume change for the reaction, respectively. The equilibrium constant of reaction (1) is defined as:

$$K = \frac{a_{fs}^5 a_{tr}^2}{a_{en}^5 a_{fact}^2} \quad (3)$$

where a_i denotes activity of component i. The value of ΔV of the reaction (1) is negative and larger than −0.2 J/bar for a wide range of P–T conditions based on the dataset of Holland and Powell (1998), indicating that the isopleth has a steep Clapeyron slope. The pressure condition of the corona formation is poorly constrained. Nevertheless, the estimated temperatures of the other pairs do not differ by 10 °C for pressures between 0.001 and 1.0 GPa. Therefore we assume pressure at the corona formation as 0.5 GPa, being the same as that of equilibrium condition of the Cam–Opx domain. The dataset of Holland and Powell (1998) provides ΔS as −83.61 J/K at 0.5 GPa and 850 °C where the entropy of ferroactinolite has been raised by 30 J/K as recommended by Dale et al. (2000). The value of ΔS varies less than 8% over the range from 0.001 to 1.0 GPa and from 500 to 1000 °C, which is less than 18.9 J/K, the standard deviation in estimating ΔS based on Einstein and Debye models (Holland, 1989). Treating ΔS to be constant and P_1 as P_0, and rearranging Eq. (2) yield:

$$T_1 = \frac{R\ln K_{P_0,T_0} - \Delta S}{R\ln K_{P_1,T_1} - \Delta S}T_0 \quad (4)$$

The equilibrium constant is a function of not only the composition of minerals but also the temperature depending on the activity models. Substituting the compositions of calcic amphibole and orthopyroxene of other pairs into Eq. (3) provides its equilibrium constant, K_{P_1,T_1}, as a function of temperature. Solution of Eqs (3) and (4) by successive approximation yields the temperature of the pairs T_1.

The present calculation, the integrated formulation of the Gibbs method (Spear et al., 1982), has two advantages in terms of the uncertainties in estimating temperature as compared with the conventional thermodynamic calculations using internally consistent datasets. Firstly, this

method does not involve enthalpy of the reaction. The standard deviation of enthalpy of the reaction (1) is 10.85 kJ using the dataset of Holland and Powell (1998), which corresponds to uncertainty in estimated temperature of 130 °C at 850 °C. Eq. (4) excludes this uncertainty from estimating T_1. Secondly, the uncertainties in ΔS provide less influence to the estimated temperature in this method as compared with the conventional calculations. The uncertainties in T_1 derived from the standard deviation of ΔS estimation (18.9 J/K) increase with increasing difference between T_0 and T_1 but do not exceed 40 °C for analyses in this study, while the conventional calculations cause uncertainties as large as 100 °C, which is comparable to those derived from enthalpy uncertainties.

This method involves an additional source of uncertainties that is derived from estimation of T_0. The metamorphic temperatures based on geothermobarometry range from 800 to 900 °C, suggesting the uncertainties of T_0 as 50 °C (Owada et al., 2005). Change of T_0 by 50 °C causes change of resultant T_1 that decreases with decreasing T_1, i.e., 50–55 °C at $T_1 > 800$ °C and 30 °C at $T_1 = 600$ °C. In total, the uncertainties of T_1 derived from those of ΔS and T_0 do not exceed 60 °C in this study, which is comparable to those of conventional geothermometry.

The equilibrium constant depends on the choice of activity models of calcic amphibole and orthopyroxene. We examined three models for orthopyroxene: one is the simplest model of ideal mixing-on-site (model 1), as employed for geothermometers (e.g., Harley, 1984). The second model is proposed by Holland and Powell (1998) who assume equipartitioning of Fe and Mg between M1 and M2 sites together with regular solution model (model 2). The third model takes partitioning of Fe and Mg between M1 and M2 sites into account and applies a regular solution model (model 3) (Holland and Powell, 1996; Powell and Holland, 1999). For calcic amphibole, the model of Dale et al. (2000) was employed that applied a regular solution model based on the assumption of equipartitioning of Fe and Mg among M13, M2 and M4 sites. Ideal mixing-on-site model for calcic amphibole was not used in this study because it yields low temperatures for pairs in the tremolite zone inconsistent with respect to the stability of orthopyroxene.

4. Temperature of the corona formation

Table 5 shows results of the calculation. The models 1 and 2 for orthopyroxene provide similar temperatures. The model 3 represents consistent but slightly higher temperatures by 20–40 °C than the former two models for the pairs in the tremolite zone. Taking average of the three calculations shows that the pairs of calcic amphibole and orthopyroxene in the Cam–Opx domain represent high temperatures as 820–880 °C, consistent with the estimated temperature by Owada et al. (2005). In contrast, the pairs in the tremolite zone represent lower temperatures as 600–710 °C (Table 5).

Introduction of ferric iron into calcic amphibole increases the equilibrium constant of both the reference pair and other pairs. The pairs in the Cam–Opx domain yield only a small change in the estimated temperature, i.e., less than 15 °C provided that the half of total iron is ferric. The estimated temperatures of the pairs in the tremolite zone, in contrast, increase with increasing the ferric content, approximately by 13 °C per 10% increase of ferric content. Therefore the ferric-free assumption accepted in this study provides the lower limit in temperature of the reaction (1) recorded in the tremolite zone. We obtain the same conclusion that the tremolite zone was equilibrated at a temperature significantly lower than the Cam–Opx domain even if we assume half of total iron to be ferric in calcic amphiboles.

The low-temperature limit of the coexistence of calcic amphibole and orthopyroxene may be defined by the stability of orthopyroxene relative to anthophyllite and olivine shown as:

$$9\ \underset{\text{orthopyroxene}}{Mg_2Si_2O_6} + 2\ \underset{\text{fluid}}{H_2O} = 2\ \underset{\text{olivine}}{Mg_2SiO_4} + 2\ \underset{\text{anthophyllite}}{Mg_7Si_8O_{22}(OH)_2} \quad (5)$$

The equilibrium temperature of reaction (5) is estimated as ca. 700 °C at 0.5 GPa in the $MgO–SiO_2–H_2O$ system

Table 5
Estimated temperatures (°C)

Occurrences	Pair of analyses		Activity model			Average
			1	2	3	
Cam–Opx domain	Hbl-7	Opx-2	850	850	850	850
	Hbl-6	Opx-3	816	816	824	819
	Hbl-11	Opx-6	824	824	830	826
	Hbl-16	Opx-7	888	888	877	884
	Hbl-17	Opx-8	827	827	834	829
	Hbl-19	Opx-9	854	855	856	855
Tremolite zone	Hbl-27	Opx-13	673	673	712	686
	Hbl-28	Opx-12	686	686	716	696
	Hbl-29	Opx-14	698	697	725	707
	Hbl-32	Opx-17	588	587	609	595
	Hbl-33	Opx-16	589	588	612	596
	Hbl-43	Opx-19	641	641	663	648
	Hbl-44	Opx-18	591	590	613	598
	Hbl-48	Opx-45	662	663	702	676
	Hbl-50	Opx-44	651	651	678	660

Three activity models for orthopyroxene were employed and denoted as 1, 2 and 3. See text for details. All the calculations assume that the pair Hbl-7–Opx-2 was equilibrated at 850 °C.

(Spear, 1993). Addition of FeO into the system decreases the temperature by several tens degree (Tracy and Frost, 1991). A decrease in H_2O activity in fluid also decreases the temperature. Therefore the temperature of 700 °C is the upper-limit of reaction (5), which provides the low-temperature limit for stability of orthopyroxene and calcic amphibole. The absence of orthoamphibole in the coronas and the estimated temperatures of 600–710 °C suggest that the corona-forming reaction took place at temperatures close to the lower limit of orthopyroxene stability.

5. Change of paragenetic relation

The following two assemblages occurring in the Ol–Pl domain are mutually incompatible in terms of isophysical variation, i.e., olivine + plagioclase + orthopyroxene + spinel, which was stable in the matrix before corona formation, and calcic amphibole + spinel in the symplectite zone. In the simplified $CaO–MgO–Al_2O_3–SiO_2–H_2O$ system, the following reaction describes the paragenetic relation between these two assemblages, which takes place at higher temperature than reaction (5).

$$\underset{\text{olivine}}{6\ Mg_2SiO_4} + \underset{\text{plagioclase}}{4CaAl_2Si_2O_8} + \underset{\text{orthopyroxene}}{Mg_2Si_2O_6} + \underset{\text{fluid}}{2H_2O} = \underset{\text{spinel}}{4\ MgAl_2O_4} + \underset{\text{tremolite}}{2Ca_2Mg_5Si_8O_{22}(OH)_2} \quad (6)$$

Two initial assemblages, i.e., olivine + plagioclase + spinel + orthopyroxene in the Ol–Pl domain and calcic amphibole + orthopyroxene in the Cam–Opx domain, can be explained as isophysical variation under conditions where the left-hand side of Eq. (6) is stable.

It is noted that Eq. (6) represents orthopyroxene as a reactant. The tschermak substitution in calcic amphibole and orthopyroxene is expressed as compositional difference between spinel and olivine such as, $Al_2Mg_{-1}Si_{-1} = MgAl_2O_4–Mg_2SiO_4$. Thus replacing tremolite and orthopyroxene in Eq. (6) by tschermakite and Tschermak pyroxene (tspx: $MgAl_2SiO_6$), respectively, yields:

$$\underset{\text{olivine}}{3Mg_2SiO_4} + \underset{\text{plagioclase}}{4CaAl_2Si_2O_8} + \underset{\text{tspx}}{MgAl_2SiO_6} + \underset{\text{fluid}}{2H_2O} = \underset{\text{spinel}}{MgAl_2O_4} + \underset{\text{tschermakite}}{2\ Ca_2Mg_3Al_4Si_6O_{22}(OH)_2} \quad (7)$$

Linear combination of Eqs. (6) and (7) provides the stoichiometric relation among these minerals with various Al content of calcic amphibole and orthopyroxene, which always treats orthopyroxene as a reactant.

These features result in that spinel and calcic amphibole in the symplectite zone were stabilized at the expense of orthopyroxene as well as olivine and plagioclase if the system was closed, which is inconsistent with the microstructural feature that orthopyroxene occurs as constituents of the corona. Furthermore, the association of olivine and plagioclase can be stable even under conditions where the right-hand side of Eq. (6) is stable, while the reaction rims occur between olivine and plagioclase. This suggests that Eq. (6) does not account well for the microstructures of the reaction rims, even though this reaction is responsible for the change of paragenetic relations before and after the corona formation.

6. Overall reaction of the corona formation

Aluminous amphibole occurs together with spinel in the symplectite zone adjacent to plagioclase and less-aluminous amphibole is associated with Al-poor orthopyroxene in the tremolite zone next to olivine, as described before. These features suggest that the former zone is more aluminous and less siliceous in bulk composition than the latter zone, while no gap in composition of calcic amphibole is recognized between the two zones. The gap in the bulk Al and Si contents between the two zones may indicate that the tremolite zone and symplectite zone were originally occupied mainly by olivine and plagioclase, respectively, and that Al and Si were approximately immobile during formation of the corona structure.

The constituent minerals are Fe^{3+}- and Na-free except for calcic amphibole in the matrix that contains a small amount of Na_2O as low as 0.8 wt.%. Ti contents of constituent minerals are negligible except for ilmenite suggesting that ilmenite did not affect significantly to the formation of the corona as a source of Ti. The formation of the corona can be therefore discussed in the $CaO–FeO–MgO–Al_2O_3–SiO_2–H_2O$ system with the assumption of immobility of Al and Si.

The formation of the tremolite zone at the expense of olivine may be expressed by a combination of the following two reactions:

$$\underset{\text{olivine (ol)}}{8\ (Mg_{0.87}Fe_{0.13})_2SiO_4} + \underset{\text{fluid}}{H_2O} + 2\ CaO = \underset{\text{tremolite (trem)}}{Ca_2(Mg_{0.92}Fe_{0.08})_5Si_8O_{22}(OH)_2} + 9.32\ MgO + 1.68\ FeO \quad (8)$$

and

$$\underset{\text{olivine (ol)}}{2\ (Mg_{0.87}Fe_{0.13})_2SiO_4} = \underset{\text{orthopyroxene (opx)}}{(Mg_{0.87}Fe_{0.13})_2Si_2O_6} + 1.74\ MgO + 0.26\ FeO \quad (9)$$

the latter of which is also responsible for the formation of orthopyroxene zone. The following reaction may account for the formation of the symplectite zone at the expense of plagioclase.

$$\underset{\text{plagioclase (pl)}}{3.75\ CaAl_2Si_2O_8} + \underset{\text{fluid}}{H_2O} + 6.52\ MgO + 1.23\ FeO = \underset{\text{magnesiohornblende (mghbl)}}{Ca_2(Mg_{0.9}Fe_{0.1})_{4.5}AlSi_{7.5}O_{22}(OH)_2} + 3.25\underset{\text{spinel (spl)}}{(Mg_{0.76}Fe_{0.24})Al_2O_4} + 1.75\ CaO \quad (10)$$

Combining Eqs. (8)–(10) so that FeO, MgO and CaO are closed in the system yields:

$$5.5\ ol + 4\ pl + opx + 2\ fluid = trem + mghbl + 3.5\ spl \quad (11)$$

which corresponds to Eq. (6) using the present compositions of minerals. Eq. (11) shows again that orthopyroxene is a reactant in the closed system and that this feature is inconsistent with the microstructures.

The area of calcic amphiboles in the tremolite zone is greater than that in the symplectite zone by a factor of ca. 1.3, which was obtained by counting number of pixel in the digitalized image of Fig. 3a. The molar volume of calcic amphiboles in both the symplectite zone and tremolite zone is similar to each other based on the dataset of Holland and Powell (1998), suggesting that the areal fraction can be regarded as the molar fraction. Summation of Eqs. (10) and (8) multiplied by 1.3 together with Eq. (9) multiplied by arbitrary number, n, yields the overall reaction as:

$$(10.4 + 2n)\ ol + 3.75\ pl + 2.3\ fluid + 0.85\ CaO = 1.3trem + mghbl + 3.25spl + n\ opx + (5.596 + 1.74n)MgO + (0.957 + 0.26n)FeO \quad (12)$$

The areal fractions of orthopyroxene and spinel with respect to calcic amphibole differ in different domains, which could not constrain the stoichiometric coefficients in reaction (12). The sign of n is required to be positive to account for the occurrence of orthopyroxene in the reaction rims. This feature indicates that the overall reaction belongs not to a closed system but to an open system that involves removal mainly of MgO together with minor removal and addition of FeO and CaO, respectively. In other word, the bulk composition of the reaction rims is different from the initial bulk composition that is represented as linear combination of olivine and plagioclase (anorthite). No reaction microstructures was recognized in the sample that released CaO and absorbed FeO and MgO, suggesting that the system was open in the scale of the rock sample.

The above argument does not deal with the formation of poikiloblasts of calcic amphibole in the matrix. The composition of the poikiloblasts changes gradually, which makes it difficult to estimate precisely the molar fraction of tremolite and magnesiohornblende. The area of the spinel-free domain in the poikiloblasts is significantly larger than that of the domain where the vermicular spinel aggretates occur. This feature may indicate that the amount of tremolite produced by the reaction (8) is larger than that of magnesiohornblende produced by reaction (10) in the poikiloblasts. Use of Eq. (8) multiplied by any number greater than unity leads to the same conclusion that the removal mainly of MgO is responsible for the formation of orthopyroxene as constituents of the corona.

7. Evolution of the microstructures

The olivine–plagioclase association can be locally stable at temperatures below the reaction (6), as described before. It is, therefore, still ambiguous how the association of olivine and plagioclase was destabilized by the reaction (12), i.e., removal of MgO. Furthermore, it may be a natural question why two types of reaction rims were formed between olivine and plagioclase. The orthopyroxene zone comprises orthopyroxene with limited Al contents. This feature suggests that plagioclase adjacent to the orthopyroxene zone did not react with olivine significantly, as suggested by reaction (9) that involves neither fluid nor hydrous minerals. In contrast, calcic amphiboles in the tremolite zone and symplectite zone were produced by the hydration reactions (8) and (10), respectively. Supposing that the incursion of aqueous fluid was not spatially homogeneous, the amount of aqueous fluid infiltrated to the olivine–plagioclase boundary would be different in local, which may cause the formation of different types of reaction rims. To deal with the evolution of the microstructures, we constructed a qualitative chemical potential diagram in the simplified $CaO–MgO–Al_2O_3–SiO_2–H_2O$ system (Fig. 7). We assume that composition of all the phases is constant, where we treated the composition of calcic amphibole as $Ca_2Mg_{4.75}Al_{0.5}Si_{7.75}O_{22}(OH)_2$, the average of tremolite and magnesiohornblende. The slope of univariant lines is drawn arbitrarily in Fig. 7 following the Schreinemakers' rule for the sake of qualitative analyses. The temperature of T_c in Fig. 7a represents the equilibrium temperature of reaction (6).

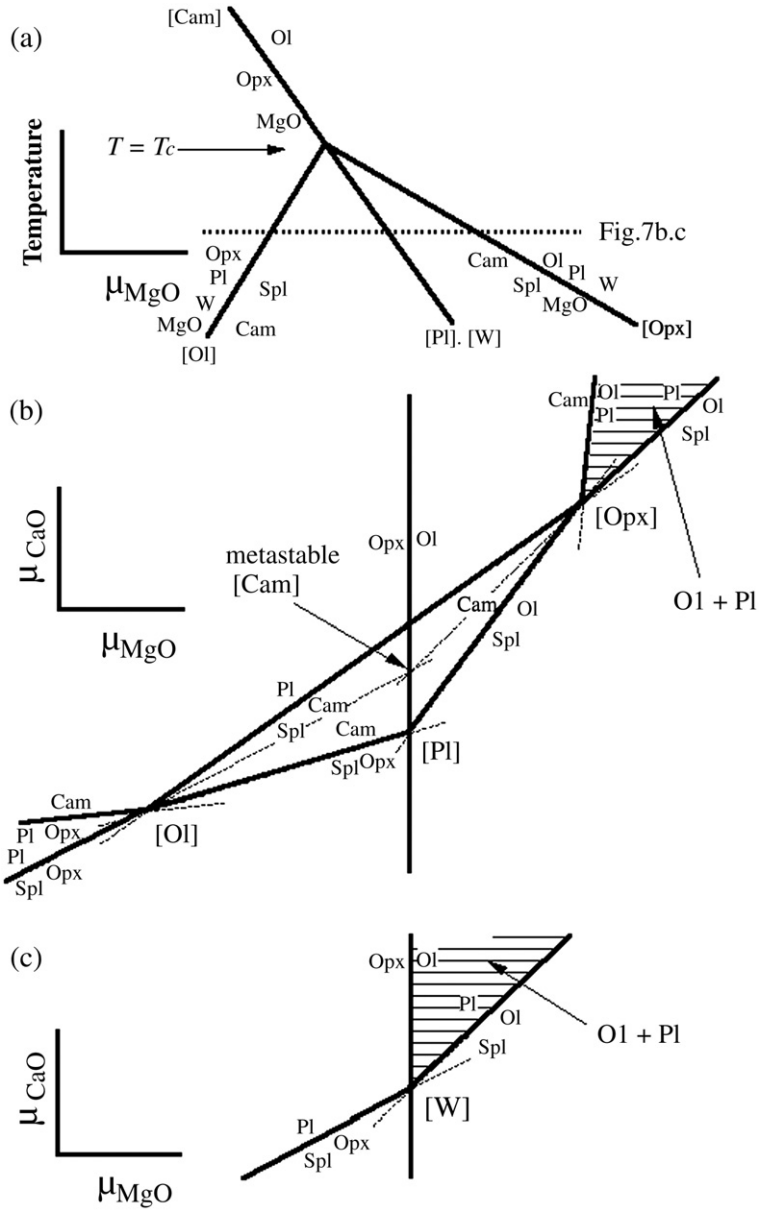


Fig. 7. Qualitative chemical potential diagram in the simplified CaO–MgO–Al_2O_3–SiO_2–H_2O system. (a) Cross section with temperature versus μ_{MgO}. (b) Isothermal cross section with μ_{CaO} versus μ_{MgO} at temperature below T_c (dotted line in a) under aqueous-fluid excess conditions. (c) Isothermal cross section at the temperature same as (b) under aqueous-fluid absent conditions. Abbreviations: Cam, calcic amphibole; Ol, olivine; Opx, orthopyroxene; Pl, plagioclase; Spl, spinel; W, aqueous fluid.

The assemblage olivine+plagioclase+orthopyroxene+spinel, stable in the Ol–Pl domain before the corona formation, is denoted as [Cam] in Fig. 7a. The chemical potential of MgO,μ_{MgO}, in the assemblage [Cam] increases with decreasing temperature, which is obtained from the Gibbs–Duhem relation. At temperatures lower than T_c, the assemblage [Cam] is unstable in the system with excess aqueous fluid but persisted metastably. Its μ_{MgO} and μ_{CaO} of the metastable assemblage [Cam] deviate from those defined by one of three possibly stable assemblages, i.e., [Opx], [Pl] or [Ol] (Fig. 7b). An increase in this chemical potential difference with decreasing temperature triggered reaction (6). The μ_{MgO} of the local association of olivine and plagioclase is the highest among the locally stable associations (Fig. 7b). Removal of MgO, probably caused by difference in μ_{MgO} between the rock and the

surroundings, would destabilize first the local association with the highest μ_{MgO} because of the largest potential gradient. This feature may be responsible for that the overall reaction (12) took place between olivine and plagioclase.

The following three local associations are recognized in the calcic amphibole-bearing reaction rims; plagioclase + spinel + calcic amphibole, spinel + calcic amphibole + orthopyroxene and olivine + orthopyroxene + calcic amphibole, the first of which has μ_{MgO} lower than the other two associations at constant μ_{CaO} (Fig. 7b). This indicates that the μ_{MgO} gradient has been maintained during the removal of MgO, which supports the validity of the assumption that the diffusion was the rate-controlling process.

Decreasing H_2O activity shifts [Ol], [Opx] and [Pl] to be close each other, and they converge to form [W] under fluid-absent conditions at the same point as metastable [Cam] (Fig. 7c). The fluid-absent condition may be applicable to the formation of the orthopyroxene zone. In Fig. 7c, the olivine–plagioclase association is destabilized by breakdown of olivine during decrease of μ_{MgO}, which is expressed as the reaction (9). Local presence or absence of aqueous fluid may be responsible for the formation of two types of reaction rims between olivine and plagioclase.

8. Conclusions

Microstructural and petrological investigations of the olivine–plagioclase corona in meta-ultramafic rocks from the Sefuri Mountains, NW Kyushu, Japan lead to the following conclusions.

Temperature of the corona formation was determined as 600–710 °C provided that the matrix had been equilibrated at 850 °C, based on the assumption of local equilibrium between calcic amphibole and orthopyroxene both in the matrix and in the corona.

The change of paragenetic relation before and after corona formation during decreasing temperature is described by Eq. (6) that sets orthopyroxene as a reactant.

The overall reaction is expressed by the open-system reaction (12) that removed mainly MgO and produced orthopyroxene as well as calcic amphibole and spinel at the expense of olivine and plagioclase. Removal of MgO is also responsible to destabilize the olivine–plagioclase association. Presence or absence of aqueous fluid at the olivine–plagioclase boundary may cause the formation of different type of the reaction rims.

It should be emphasized that the presence of orthopyroxene as a product in the corona is not always indicative of an orthopyroxene-producing reaction being responsible for the change of paragenetic relation.

Acknowledgements

This study was financially supported in part by Grant-in-Aid for Scientific Research (A) (17204045) from the Japan Society for the Promotion of Science. We are grateful to I. Buick for valued comments and editorial works.

References

Ashworth, J.R., Birdi, J.J., 1990. Diffusion modelling of coronas around olivine in an open system. Geochimica et Cosmochimica Acta 54, 2389–2401.

Ashworth, J.R., Sheplev, V.S., 1997. Diffusion modelling of metamorphic layered coronas with stability criterion and consideration of affinity. Geochimica et Cosmochimica Acta 61, 3671–3689.

Ashworth, J.R., Birdi, J.J., Emmett, T.F., 1992. A complex corona between olivine and plagioclase from the Jotun Nappe, Norway, and the diffusion modelling of multimineralic layers. Mineralogical Magazine 56, 511–525.

Dale, J., Holland, T.J.B., Powell, R., 2000. Hornblende–garnet–plagioclase thermobarometry: a natural assemblage calibration of the thermodynamics of hornblende. Contributions to Mineralogy and Petrology 140, 353–362.

Fisher, G.W., 1973. Nonequilibrium thermodynamics as a model for diffusion-controlled metamorphic processes. American Journal of Science 273, 897–924.

Fisher, G.W., 1978. Rate laws in metamorphism. Geochimica et Cosmochimica Acta 42, 1035–1050.

Grant, S.M., 1988. Diffusion models for corona formation in metagabbros from the western Grenville Province, Canada. Contributions to Mineralogy and Petrology 98, 49–63.

Grieve, R.A.F., Gittins, J., 1975. Composition and formation of coronas in the Hadlington gabbro, Ontario, Canada. Canadian Journal of Earth Sciences 12, 289–299.

Harley, S.L., 1984. An experimental study of the partitioning of Fe and Mg between garnet and orthopyroxene. Contributions to Mineralogy and Petrology 86, 359–373.

Holland, T.J.B., 1989. Dependence of entropy on volume for silicate and oxide minerals: a review and a predictive model. American Mineralogist 74, 5–13.

Holland, T.J.B., Blundy, J., 1994. Non-ideal interactions in calcic amphiboles and their bearing on amphibole–plagioclase thermometry. Contributions to Mineralogy and Petrology 116, 433–447.

Holland, T.J.B., Powell, R., 1996. Thermodynamics of order–disorder in minerals: II. Symmetric formalism applied to solid solutions. American Mineralogist 81, 1425–1437.

Holland, T.J.B., Powell, R., 1998. An internally consistent thermodynamic data set for phases of petrological interest. Journal of Metamorphic Geology 16, 309–343.

Ikeda, T., 2004. Pressure–temperature conditions of the Ryoke metamorphic rocks in Yanai district, SW Japan. Contributions to Mineralogy and Petrology 146, 577–589.

Inoue, T., 1961. Structural–petrological studies of metamorphic complex of the Seburi Mountainland, with special reference to its bearing on the metamorphism of the Sangun Metamorphic Zone in northern Kyushu. Journal of Science of the Hiroshima University, Series C 3, 403–424.

Joesten, R., 1977. Evolution of mineral assemblage zoning in diffusion metasomatism. Geochimica et Cosmochimica Acta 41, 649–670.

Johnson, C.D., Carlson, W.D., 1990. The origin of olivine–plagioclase coronas in metagabbros from the Adirondack Mountains, New York. Journal of Metamorphic Geology 8, 697–717.

Karakida, Y., 1951. Hornblende hybrids of the Iba-toge, Southwest of Fukuoka. Science Reports of Department of Geology, Kyushu University 3, 21–30 (in Japanese).

Karakida, Y., 1965. Kitazaki granodiorite and Sangun metamorphic rocks of Noko island and Kashii, Fukuoka. Studies in Literature and Science of Seinan Gakuin University 6, 19–44 (in Japanese with English abstract).

Karakida, Y., 1969. Almandine garnets from polymetamorphic hornfelses in the Iba-Raizan area, southwest of Fukuoka. Science Reports of Department of Geology, Kyushu University 9, 99–104 (in Japanese with English abstract).

Karakida, Y., 1971. Calcareous hornfelses in the Iba area, southwest of Fukuoka. Professor Hisamichi Matsushita Memorial Volume. Fukuoka Publication Co, pp. 371–380 (in Japanese with English abstract).

Karakida, Y., Tomita, S., Shimoyama, S., Chijiwa, K., 1994. Geology of the Fukuoka district. with geological sheet map at 1: 50,000, Geological Survey of Japan 192 pp. (in Japanese with English abstract).

Lamoen, H., 1979. Coronas in olivine gabbros and iron ores from Susimäki and Riuttamaa, Finland. Contributions to Mineralogy and Petrology 68, 259–268.

Leake, B.E., Woolley, A.R., Arps, C.E.S., et al., 1997. Nomenclature of amphiboles: Report of the subcommittee on amphiboles of the International Mineralogical Association, Commission on New Minerals and Mineral Names. Mineralogical Magazine 61, 295–321.

Loomis, T.P., 1976. Irreversible reactions in high-grade metapelitic rocks. Journal of Petrology 17, 559–588.

Matsumoto, T., 1958. Geology of metamorphic regions in the Chikushi Mountains. Jubilee Publication in the Commemoration of Professor Jun Suzuki, M.J.A. Sixtieth Birthday, pp. 141–161 (in Japanese).

Mongkoltip, P., Ashworth, J.R., 1983. Quantitative estimation of an open-system symplectite-forming reaction: restricted diffusion of Al and Si in coronas around olivine. Journal of Petrology 24, 635–661.

Moore, A.C., 1970. Descriptive terminology for the textures of rocks in granulite facies terrains. Lithos 3, 123–127.

Nakamura, D., 2002. Kinetics of decompressional reactions in eclogitic rocks: formation of plagioclase coronas around kyanite. Journal of Metamorphic Geology 20, 325–333.

Nishimura, Y., 1998. Geotectonic subdivision and areal extent of the Sangun belt, Inner zone of southwest Japan. Journal of Metamorphic Geology 16, 129–140.

Nishiyama, T., 1983. Steady diffusion model for olivine–plagioclase corona growth. Geochimica et Cosmochimica Acta 47, 283–294.

Owada, M., Jikihara, S., Osanai, Y., Yamamoto, K., 2000. Low P/T metamorphic rocks from Sefuri Mountains and its correlation with low P/T type metamorphic rocks in Kyushu, southwest Japan. Memoir of the Geological Society of Japan 56, 229–240 (in Japanese with English abstract).

Owada, M., Hada, R., Yada, J., Nakamura, M., Osanai, Y., 2005. Newly found granulites from the western part of Sefuri Mountains, North Kyushu. Journal of the Geological Society of Japan 111, 50–53 (in Japanese with English abstract).

Powell, R., Holland, T.J.B., 1999. Relating formulations of the thermodynamics of mineral solid solutions: activity modeling of pyroxenes, amphiboles, and micas. American Mineralogist 84, 1–14.

Spear, F.S., 1993. Metamorphic phase equilibria and pressure–temperature-time paths. Mineralogical Society of America Monograph, Washington DC.

Spear, F.S., Ferry, J.M., Rumble III, D., 1982. Analytical formulation of phase equilibria: the Gibbs method. In: Ferry, J.M. (Ed.), Characterization of metamorphism through mineral equilibria. Review in Mineralogy, vol. 10. Mineralogical Society of America, Washington DC, pp. 105–152.

Sugi, K., 1951. Metablastic rocks associated with amphibolites from the Northern Slope of the Seburi Mountainland, North Kyushu. Science Reports of Department of Geology, Kyushu University 3, 13–20 (in Japanese).

Tracy, R.J., Frost, B.R., 1991. Phase equilibria and thermobarometry of calcareous, ultramafic and mafic rocks, and iron formations. In: Kerrick, D.M. (Ed.), Contact metamorphism. Review in Mineralogy, vol. 26. Mineralogical Society of America, Washington DC, pp. 207–290.

Yamada, S., Yanagi, T., 1986. High-grade metamorphic rocks in the Itoshima granodiorites, North Kyushu. Abstract of annual meeting of the Japanese association of Mineralogists, Petrologists and Economic Geologists, vol. 81, pp. 148–149 (in Japanese).